

## Oxidation-induced crack healing in $\text{Ti}_3\text{AlC}_2$ ceramics

G.M. Song,<sup>a,\*</sup> Y.T. Pei,<sup>b</sup> W.G. Sloof,<sup>c</sup> S.B. Li,<sup>d</sup> J.Th.M. De Hosson<sup>b</sup> and  
S. van der Zwaag<sup>a</sup>

<sup>a</sup>*Fundamentals of Advanced Materials, Faculty of Aerospace Engineering, Delft University of Technology,  
Kluyverweg 1, 2629 HS Delft, The Netherlands*

<sup>b</sup>*Department of Applied Physics, The Netherlands Institute for Metals Research, University of Groningen, Nijenborgh 4,  
9747 AG Groningen, The Netherlands*

<sup>c</sup>*Department of Materials Science and Engineering, Delft University of Technology, Mekelweg 2, 2628 CD Delft, The Netherlands*

<sup>d</sup>*Materials Engineer Center, Beijing Jiaotong University, Beijing 100044, China*

Received 27 August 2007; accepted 4 September 2007

Available online 1 October 2007

Crack healing of  $\text{Ti}_3\text{AlC}_2$  was investigated by oxidizing a partially pre-cracked sample. A crack near a notch was introduced into the sample by tensile deformation. After oxidation at 1100 °C in air for 2 h, the crack was completely healed, with oxidation products consisting primarily of  $\alpha\text{-Al}_2\text{O}_3$  as well as some rutile  $\text{TiO}_2$ . The indentation modulus and hardness of the crack-healed zone are slightly higher compared with those of the  $\text{Ti}_3\text{AlC}_2$  base material. The preferential oxidation of Al atoms in  $\text{Ti}_3\text{AlC}_2$  grains on the crack surface results in the predominance of  $\alpha\text{-Al}_2\text{O}_3$  particles forming in a crack less than 1  $\mu\text{m}$  wide.

© 2007 Acta Materialia Inc. Published by Elsevier Ltd. All rights reserved.

**Keywords:** Crack healing;  $\text{Ti}_3\text{AlC}_2$ ; High-temperature oxidation; Preferential oxidation; Mechanical property

Crack healing in ceramic materials via surface oxidation or thermal diffusion has been well documented in the literature [1–8]. The oxidation mechanism [1–5] exhibits better healing efficiency than the diffusion mechanism because the volume expansion induced by crack surface oxidation can effectively fill the crack opening, whereas the diffusion mechanism relies on the mass flux from the base material to the crack zone [6–8]. In the past 20 years, investigation into crack-healing in engineering ceramics has mainly concentrated on  $\text{SiC}$  and  $\text{Si}_3\text{N}_4$  and their composites because their microcracks can be effectively healed with high-temperature oxidation products such as  $\text{SiO}_2$  [1–5]. The good crack-healing ability undoubtedly increases the reliability and competitive potential of these ceramics as high-temperature structural components.

The recently developed ternary carbide  $\text{Ti}_3\text{AlC}_2$  has an excellent combination of properties of both ceramics and metals, and is a very promising material for high-temperature applications [9–15]. Given the potential application of  $\text{Ti}_3\text{AlC}_2$  ceramics at high temperatures,

it would be very attractive if damage to  $\text{Ti}_3\text{AlC}_2$  ceramics could be healed autonomously during service at a high operating temperatures. Information about the crack-healing ability of  $\text{Ti}_3\text{AlC}_2$  ceramics, which has not yet been reported in literature, will be the topic of this paper.

The present work concentrates on the crack-healing ability of  $\text{Ti}_3\text{AlC}_2$  in a high-temperature oxidizing environment. A crack in a  $\text{Ti}_3\text{AlC}_2$  sample was created by tensile loading. The cracked sample was then exposed to high temperatures in an oxidizing environment to heal the crack. The mechanical properties of healed crack zone were evaluated using nanoindentation.

The  $\text{Ti}_3\text{AlC}_2$  bulk sample was prepared by an in situ solid-liquid reactive hot-pressing method. Ti, Al and graphite powders with the desired atomic ratio of 3:1.1:2 were mixed by ball-milling for 4 h in an ethanol solution. The slurry was dried at 60 °C and cold-pressed into blocks in a graphite die under 8 MPa, and then hot-pressed at 1425 °C under 20 MPa for 30 min in flowing argon gas. The final dimensions of these  $\text{Ti}_3\text{AlC}_2$  blocks were  $35 \times 25 \times 5 \text{ mm}^3$ .

In order to introduce a crack in  $\text{Ti}_3\text{AlC}_2$  ceramics in a controllable manner, a  $\text{Ti}_3\text{AlC}_2$  specimen  $8 \times 2 \times 0.3 \text{ mm}^3$  was glued onto a steel tensile bar, as sketched in

\* Corresponding author. Tel.: +31 15 2781607; fax: +31 15 2784472;  
e-mail: [g.song@tudelft.nl](mailto:g.song@tudelft.nl)

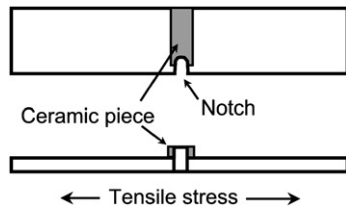


**Figure 1.** Sketch showing the method used to make a single edge notch and microcrack in a  $\text{Ti}_3\text{AlC}_2$  specimen bonded to a steel tensile bar.

**Figure 1.** A notch was made on one side of the ceramic piece and the steel bar with a saw. The depth of the notch in the  $\text{Ti}_3\text{AlC}_2$  piece and the steel bar was 0.5 and 2.5 mm, respectively. Next, the tensile bar was mounted on a micro tensile stage (Deben Micro Tensile Device-5KN) installed in a scanning electron microscope (SEM, JEOL JSM 6500F). Tensile load was applied to the bar until a crack was initiated near the center of the notch in the  $\text{Ti}_3\text{AlC}_2$  specimen, which was monitored with SEM observations. Thereafter, the sample was unloaded.

The cracked ceramic piece was removed from the steel bar by dissolving the glue in acetone for 24 h, and was thoroughly cleaned twice with isopropanol. The sample was heated at 1100 °C for 2 h in air.

The microstructures of the sample were studied via the JSM 6500F-SEM equipped with an energy dispersive spectrometer (EDS). The crystalline phases present in the sample before and after heat treatment were identified by X-ray diffractometry (XRD) using a Bruker AXS D5005. An MTS Nano Indenter XP equipped with a Berkovich indenter was used to measure the indentation modulus ( $E$ ) and hardness ( $H$ ) on the local healed zone. The averaged values of  $E$  and  $H$  were obtained over a range of indentation depth of 60–150 nm.

A crack with a length of  $\sim 7$  mm in the  $\text{Ti}_3\text{AlC}_2$  sample is shown in Figure 2a. Once the crack had been nucleated, it propagated rapidly perpendicular to the

tensile loading direction. The average width of the crack is about 5  $\mu\text{m}$ . Images at higher magnification (Fig. 2 inset) show that the crack propagates in a zigzag mode so as to follow the basal planes of the hexagonal  $\text{Ti}_3\text{AlC}_2$  randomly oriented lamellar grains. This zigzag crack pattern in combination with local crack bridging is responsible for the high toughness of the ceramic material ( $K_{\text{IC}} \sim 8 \text{ MPa m}^{1/2}$ ).

The crack was invisible after oxidation treatment at 1100 °C for 2 h because an oxide layer covered the sample. After removing the oxide scale of the sample by mechanical polishing, it was found that the crack was fully healed, i.e. filled with oxidation products as shown in Figure 2b. Elemental Ti, Al and O maps of the healed crack zone show that high Al content bands adjacent to the  $\text{Ti}_3\text{AlC}_2$  base material are always accompanied by high O content and low Ti content. EDS analysis reveals that the crack opening has been filled by two  $\text{Al}_2\text{O}_3$  layers adjacent to the crack surfaces and a  $\text{TiO}_2$  layer in between (see Fig. 3). An interesting observation is that when the crack opening is less than 1  $\mu\text{m}$ , the filling materials consist mainly of  $\text{Al}_2\text{O}_3$ . For instance, the composition of the narrowest filled crack (point A, see Fig. 4) on the cross-section of a healed sample is 62 at.% O, 31 at.% Al and 7 at.% Ti. As the crack width increases, the  $\text{TiO}_2$  content becomes higher. For instance, the composition at point A in Figure 3 is 51 at.% O, 20 at.% Al and 31 at.% Ti.

To explore the crack-healing mechanism, the oxidation behavior of  $\text{Ti}_3\text{AlC}_2$  ceramic was investigated by a stepwise oxidation procedure of the fracture surface, as shown in Figure 5. First, a thin continuous oxide scale consisting of nanosized particles covered the fracture surface after oxidation for 180 s (Fig. 5a). The oxide scale then grew with nanosized faceted particles on top when the oxidation time was prolonged to 360 s (Fig. 5b). The faceted particles grew further and the oxide scale thickened with time. After oxidizing for 900 s, the mean size of the faceted particles increased

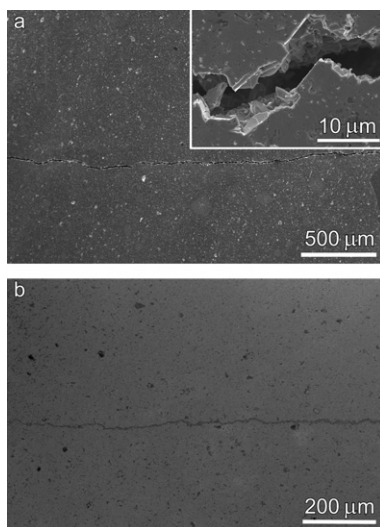


**Figure 2.** (a) A crack with a length of  $\sim 7$  mm and an average width of 5  $\mu\text{m}$  introduced into the  $\text{Ti}_3\text{AlC}_2$  sample. The inset is a higher-magnification image of the crack. (b) A healed crack.

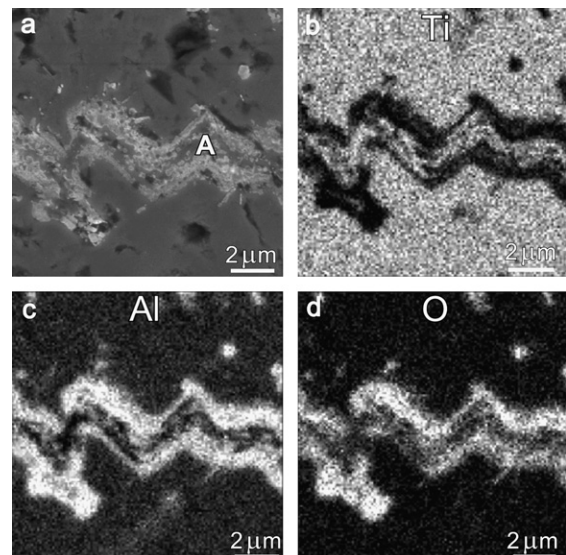


**Figure 3.** Cross-section of the healed  $\text{Ti}_3\text{AlC}_2$  sample. (a) SEM image; (b) Ti map; (c) Al map; (d) O map.

Download English Version:

<https://daneshyari.com/en/article/1503196>

Download Persian Version:

<https://daneshyari.com/article/1503196>

[Daneshyari.com](https://daneshyari.com)